ELSEVIER

Comput. Methods Appl. Mech. Engrg. 176 (1999) 313–331

Computer methods in applied mechanics and engineering

www.elsevier.com/locate/cma

On goal-oriented error estimation for elliptic problems: application to the control of pointwise errors

S. Prudhomme[1], J.T. Oden*

Texas Institute for Computational and Applied Mathematics, The University of Texas at Austin, SHC 304, 105 W. Dean Keeton St., Austin, TX 78712, USA

Abstract

A method to estimate and control pointwise errors in finite element approximations of elliptic problems is presented as an application of the more general theory of goal-oriented error estimation. In the latter, the accuracy of numerical approximations is assessed in terms of measures that are of practical interest to engineers rather than the classical global energy norm. Goal-oriented error estimation requires the solution of a problem dual to the original problem and the computation of several global error estimates. The performance of the method is carefully tested in the particular case of estimation and control of pointwise errors on a one-dimensional problem.

1. Introduction

A posteriori error estimation in finite element analysis has proven to be essential towards the design of reliable adaptive methods to improve the efficiency of simulations. However, the effort so far has focused on the development of techniques to estimate the error in the classical global energy norm based on residual methods (see [1–3,7,6,19]) or on recovery methods (see [20,21]). Although these techniques have been shown to be reliable and robust in many applications, the error measured in the energy norm brings very little relevant information to the engineers about accuracy, especially when simulations are run with a specific goal in mind, like evaluating the temperature or the stress at a given critical point in the domain.

In recent years, alternative methods have been proposed to estimate and control the numerical error with respect to measures other than the usual energy norm (see [9,8,18,15,17,4]). These measures are expressed in terms of a linear functional of the solution and generally represent a physical quantity of practical interest to engineers and designers. This new approach in a posteriori error estimation is referred to here as *goal-oriented error estimation*. In this paper, the theory of goal-oriented error estimation is presented in a simple, general and rigorous way for the case of elliptic problems. It involves the computation of an *influence function* for each quantity of interest. The influence function, obtained as the solution of a dual problem, indicates how the residual, i.e. the source of errors, influences the error in the particular measure. We also show how to estimate lower and upper bounds of the error in the goal using global energy error estimates.

In goal-oriented error estimation, the user has a lot of freedom in defining the quantity of interest. There are actually many choices depending on the specific goal, so we decide here to concentrate on pointwise error estimation. One of the major issues that needs to be addressed is that the solution and/or its derivatives may not

* Corresponding author. Director, TICAM, Cockrell Family Regents Chair in Engineering.

[1] Graduate Research Assistant.

0045-7825/99/$ – see front matter
PII: S0045-7825(98)00343-0

be continuous for certain applications so that these quantities may not be defined at certain points of the computational domain. We propose to circumvent this particular problem by defining a linear functional using the *mollification* technique. Mollification can be viewed as an averaging of the solution over a small neighborhood of the point of interest.

Following the introduction, we present a model problem and some relevant notations in Section 2. We provide in Section 3 a detailed account on global error estimation with respect to the energy norm. We actually describe how to derive lower and upper bounds of the error as these will be employed in goal-oriented error estimation. The presentation of the goal-oriented error estimation theory follows in Section 4, along with its application to the case of pointwise error estimation. We propose, in Section 5, an adaptation strategy for finite element meshes aimed at controlling and reducing pointwise errors. Finally, the method is applied to a one dimensional example with the numerical results recounted in Section 6, followed by a summary of our major conclusions.

2. Preliminaries

For the presentation of the theory, we consider an abstract model problem. Let Ω denote an open bounded domain of $\mathbb{R}^d$, with boundary $\partial\Omega$. V is assumed to be a Hilbert space of functions defined on Ω. The model problem consists of finding a function $u \in V$ which satisfies:

$$B(u, v) = F(v), \quad \forall v \in V. \tag{2.1}$$

Here, $B(\cdot, \cdot)$ designates a symmetric positive-definite bilinear form on $V \times V$, and thus defines an inner product on V. The associated norm, commonly called the *energy norm*, is denoted $\|\cdot\|_e$. The loading F is an element of the dual space V'. We note that the boundary conditions satisfied by u on $\partial\Omega$ are implicitly included in the definitions of the space V or the loading F. Then, from the Lax–Milgram theorem, we know that such a problem admits a unique solution $u \in V$.

In order to approximate the solution u, one may construct a finite element space $V^{h,p} \subset V$ of hierarchical piecewise polynomial functions, where h and p refer to the size and maximal degree of the shape functions for each element, respectively (see e.g. [10]). The mesh, formed by the union of all elements, is assumed to coincide exactly with the domain Ω. By the classical Galerkin method, one obtains a finite element solution $u_{h,p} \in V^{h,p}$ by solving the finite system of equations:

$$B(u_{h,p}, v) = F(v), \quad \forall v \in V^{h,p}. \tag{2.2}$$

The numerical error in the finite element solution $u_{h,p}$ is simply $e = u - u_{h,p}$. It belongs to the space V and, replacing u by $u_{h,p} + e$ in (2.1), is shown to be governed by the equation:

$$B(e, v) = \mathcal{R}^u_{h,p}(v), \quad \forall v \in V, \tag{2.3}$$

where $\mathcal{R}^u_{h,p}$ is called the *residual*:

$$\mathcal{R}^u_{h,p}(v) = F(v) - B(u_{h,p}, v), \quad v \in V. \tag{2.4}$$

The residual is a linear functional in V' defined in terms of the loading F and the finite element solution $u_{h,p}$. It can be interpreted as the source of the errors. One immediately notices that $\mathcal{R}^u_{h,p}(v) = 0$, $\forall v \in V^{h,p}$, which yields the well-known *orthogonality property* for the error:

$$B(e, v) = 0, \quad \forall v \in V^{h,p}. \tag{2.5}$$

The orthogonality property simply means that the finite element solution $u_{h,p}$ is the best approximation in $V^{h,p}$ of the exact solution u with respect to the energy norm $\|\cdot\|_e$. The goal in a posteriori error estimation is to postprocess the residual in order to derive, in an inexpensive manner, relevant measures of the error e.

3. Global error estimation

In this section, we present the methodology to calculate lower and upper bounds on the error in the energy norm by the *residual approach*. First, we define the norm of the residual in the dual space V' as

$$\|\mathcal{R}^u_{h,p}\|_* = \sup_{v\in V\setminus\{0\}} \frac{|\mathcal{R}^u_{h,p}(v)|}{\|v\|_e} \tag{3.1}$$

which allows us to establish the following equality

$$\|e\|_e = \|\mathcal{R}^u_{h,p}\|_* . \tag{3.2}$$

Therefore, it suffices to compute the norm of the residual to obtain the error in the energy norm. By applying the *Riesz Representation theorem*, we know that there exists a unique function $\varphi \in V$ which satisfies $\|\mathcal{R}^u_{h,p}\|_* = \|\varphi\|_e$ and:

$$B(\varphi, v) = \mathcal{R}^u_{h,p}(v), \quad \forall\, v \in V . \tag{3.3}$$

Obviously, because of the uniqueness of the solution to (2.3), the function φ is simply the error e. However, we intentionally retain the notation φ since the functions φ and e are not necessarily identical in the case of more complicated problems, for instance the Stokes problem (see [13]). Note that the problem for φ is infinite dimensional, which implies that only approximations of φ, and a fortiori of the norm of the residual, can be sought. In order to derive lower and upper bounds on $\|e\|_e$, the basic approach would be to construct two adequate spaces V_- and V_+, $V_- \subseteq V \subseteq V_+$, so that

$$\sup_{v\in V_-\setminus\{0\}} \frac{|\mathcal{R}^u_{h,p}(v)|}{\|v\|_e} \leqslant \|\mathcal{R}^u_{h,p}\|_* \leqslant \sup_{v\in V_+\setminus\{0\}} \frac{|\mathcal{R}^u_{h,p}(v)|}{\|v\|_e} \tag{3.4}$$

provided that one can find a proper extention of $\mathcal{R}^u_{h,p}$ to the space V_+. The space V is an infinite dimensional space, so it is actually impossible to construct a space V_+ of finite dimension that contains V. Nevertheless, one can compute a true upper bound with respect to a finite element approximation of the norm of the residual.

3.1. Approximation of the norm of the residual

Let $\tilde{V}^{h,p} \subset V$ be a finite element space in which one seeks an approximation $\tilde{\varphi}$ of φ satisfying:

$$B(\tilde{\varphi}, v) = \mathcal{R}^u_{h,p}(v), \quad \forall\, v \in \tilde{V}^{h,p} . \tag{3.5}$$

The energy norm of $\tilde{\varphi}$ is then given by:

$$\|\tilde{\varphi}\| = \sup_{v\in \tilde{V}^{h,p}\setminus\{0\}} \frac{|\mathcal{R}^u_{h,p}(v)|}{\|v\|_e} . \tag{3.6}$$

Combining (3.3) and (3.5), one observes that

$$B(\varphi - \tilde{\varphi}, \tilde{\varphi}) = 0 .$$

In other words, $\tilde{\varphi}$ is the orthogonal projection of φ onto the finite element space $\tilde{V}^{h,p}$ with respect to the inner product $B(\cdot,\cdot)$. It immediately follows that

$$\|\varphi\|_e^2 = \|\varphi - \tilde{\varphi}\|_e^2 + \|\tilde{\varphi}\|_e^2 . \tag{3.7}$$

Assuming there exists $v \in \tilde{V}^{h,p}$ such that $\mathcal{R}^u_{h,p}(v) \neq 0$, implying $\|\tilde{\varphi}\|_e \neq 0$, then from (3.7), one can find σ, $0 \leqslant \sigma < 1$, such that

$$\|\varphi - \tilde{\varphi}\|_e = \sigma \|\varphi\|_e . \tag{3.8}$$

In other words, the constant σ determines the relative error in the numerical approximation $\tilde{\varphi}$. Then, using (3.8) in (3.7), one obtains

$$\|\varphi\|_e^2 = \sigma^2\|\varphi\|_e^2 + \|\tilde{\varphi}\|_e^2$$
$$(1-\sigma^2)\|\varphi\|_e^2 = \|\tilde{\varphi}\|_e^2$$

that is

$$\|\tilde{\varphi}\|_e = \sqrt{1-\sigma^2}\|\varphi\|_e = \sqrt{1-\sigma^2}\|\mathcal{R}^u_{h,p}\|_* . \tag{3.9}$$

This result reveals that even a crude approximation $\tilde{\varphi}$ of φ still provides an acceptable estimate of $\|\mathcal{R}^u_{h,p}\|_*$. Indeed, even a relative error $\sigma = 30\%$ would allow to estimate $\|\mathcal{R}^u_{h,p}\|_*$ with an effectivity greater than 95%. Supposing that one can find a good approximation $\tilde{\varphi}$ of φ, in the sense that σ is 'sufficiently small', then V_- and V_+ should satisfy $V_- \subseteq \tilde{V}^{h,p} \subseteq V_+$ in order to obtain:

$$\sup_{v\in V_-\setminus\{0\}} \frac{|\mathcal{R}^u_{h,p}(v)|}{\|v\|_e} \leqslant \|\tilde{\varphi}\|_e \leqslant \sup_{v\in V_+\setminus\{0\}} \frac{|\mathcal{R}^u_{h,p}(v)|}{\|v\|_e} . \tag{3.10}$$

3.2. Lower bounds

In the previous section, we assumed that the enriched finite element space $\tilde{V}^{h,p}$ is chosen so that the action of $\mathcal{R}^u_{h,p}$ is different from 0 on at least one element of $\tilde{V}^{h,p}$. Because the residual is identically 0 on $V^{h,p}$ when u is the solution of the finite element problem (2.2), we want $V^{h,p} \subsetneq \tilde{V}^{h,p}$. Let $\tilde{V}^{h,p}$ be constructed by enriching $V^{h,p}$ with elements of a finite element space W that satisfies

$$W \neq \{0\}, \qquad W \cap V^{h,p} = \{0\}, \qquad \tilde{V}^{h,p} = W + V^{h,p} .$$

Here, we also take advantage of the residual vanishing on $V^{h,p}$ by considering the function $\psi \in W$ such that

$$B(\psi, v) = \mathcal{R}^u_{h,p}(v), \quad \forall\, v \in W . \tag{3.11}$$

Following Bank [5], one recognizes that the *strengthened Cauchy–Schwartz inequality* holds with respect to the spaces $V^{h,p}$ and W, in the sense that, for all $v \in V^{h,p}$ and $w \in W$ there exists a constant γ, $0 \leqslant \gamma < 1$, such that

$$|B(v,w)| \leqslant \gamma\|v\|_e\|w\|_e . \tag{3.12}$$

This follows from the property $W \cap V^{h,p} = \{0\}$. Eq. (3.12), along with Young's inequality, implies that

$$\begin{aligned}\|v+w\|_e^2 &= \|v\|_e^2 + 2B(v,w) + \|w\|_e^2 \\ &\geqslant \|v\|_e^2 - 2\gamma\|v\|_e\|w\|_e + \|w\|_e^2 \\ &\geqslant \|v\|_e^2 - \|v\|_e^2 - \gamma^2\|w\|_e^2 + \|w\|_e^2 \\ &\geqslant (1-\gamma^2)\|w\|_e^2 ,\end{aligned}$$

thus

$$\|v+w\|_e \geqslant \sqrt{1-\gamma^2}\|w\|_e . \tag{3.13}$$

Then, the accuracy of the approximation ψ of $\tilde{\varphi}$ can be quantified as follows:

THEOREM 3.1. Let $\tilde{\varphi} \in \tilde{V}^{h,p}$ and $\psi \in W$ be the solutions of (3.5) and (3.11), respectively, where $\tilde{V}^{h,p}$ and W are defined above. Then, there exists a constant γ such that $0 \leqslant \gamma < 1$ and

$$\sqrt{(1-\gamma^2)}\|\tilde{\varphi}\|_e \leqslant \|\psi\|_e \leqslant \|\tilde{\varphi}\|_e . \tag{3.14}$$

PROOF. The upper bound is readily obtained since $W \subset \tilde{V}^{h,p}$. In order to prove the lower bound, we set $\tilde{\varphi} = v^* + w^*$, where v^* and w^* are elements of $V^{h,p}$ and W, respectively. Now, from (3.5)

$$\|\tilde{\varphi}\|_e^2 = B(\tilde{\varphi}, \tilde{\varphi}) = \mathcal{R}^u_{h,p}(\tilde{\varphi}) = \mathcal{R}^u_{h,p}(v^*) + \mathcal{R}^u_{h,p}(w^*) . \tag{3.15}$$

Since $v^* \in V^{h,p}$, $\mathcal{R}^u_{h,p}(v^*) = 0$ and from (3.11), $\mathcal{R}^u_{h,p}(w^*) = B(\psi, w^*)$. Therefore,

$$\|\tilde{\varphi}\|_e^2 = B(\psi, w^*) \leq \|\psi\|_e \|w^*\|_e . \tag{3.16}$$

Using the strengthened Cauchy–Schwartz inequality, there exists γ, $0 \leq \gamma < 1$, such that

$$\|\tilde{\varphi}\|_e^2 \leq \frac{1}{\sqrt{1-\gamma^2}} \|\psi\|_e \|v^* + w^*\|_e = \frac{1}{\sqrt{1-\gamma^2}} \|\psi\|_e \|\tilde{\varphi}\|_e , \tag{3.17}$$

that is,

$$\sqrt{1-\gamma^2}\|\tilde{\varphi}\|_e \leq \|\psi\|_e . \tag{3.18}$$

The lower bound is proved. □

It immediately follows from (3.14) and (3.9) that

$$\sqrt{(1-\sigma^2)(1-\gamma^2)}\|\varphi\|_e \leq \|\psi\|_e \leq \|\varphi\|_e . \tag{3.19}$$

The above inequalities reveal that the approximation $\|\psi\|_e$ is always a lower bound of $\|\tilde{\varphi}\|_e$ and $\|\varphi\|_e$. The accuracy, however, depends on the unknown constants σ and γ. The former is related to the 'richness' of the space $\tilde{V}^{h,p}$, or W, in the sense that σ tends to zero as more and more degrees of freedom are added to the space $\tilde{V}^{h,p}$. On the other hand, the constant γ represents a measure of the angle between the spaces W and $V^{h,p}$. For example, in the case where W is orthogonal to $V^{h,p}$ with respect to the inner product $B(\cdot,\cdot)$, the constant γ is simply equal to zero. Consequently, its value is directly dependent on the choice of the basis functions used to construct W and $V^{h,p}$.

The choice of the space W is clearly not unique and is governed by the *trade-off between cost and accuracy*. Indeed, for high accuracy, it is desirable that W contain a lot of degrees of freedom, but this in turn would result in a prohibitively expensive problem (3.11). Some of the choices for constructing W are

(1) In the h-approach, one divides each element of the mesh into subelements of the same p order. The basis functions introduced by these smaller elements, less the basis functions of $V^{h,p}$, make up the space W. This approach is used by Huerta et al. [11].

(2) In the p-approach, the space W is conveniently constructed from layers of piecewise polynomial basis functions involving polynomials of degree between $p+1$ and $p+q$, $q \geq 1$. These basis functions are commonly called *bubble* functions or simply *bubbles*. The distribution of q over the elements is usually chosen to be uniform, i.e. $q = 1$ or 2, but we advocate an adaptive search for q. In two-dimensional problems for example, the space W can consist, as a first guess, of 'edge' bubbles of degree $q = 1$. Then, it can be successively enriched with 'interior' and 'edge' bubbles of higher degree in the elements where we have large contributions to the previous global estimates. Such an approach has been successfully used in [13] for the Stokes problem.

Here, we favor the p-approach to construct the space W. And, in order to solve the global problem (3.11) in an inexpensive manner, we use the Conjugate-Gradient method performing only a few iterations. The error estimator is then denoted:

$$\eta^u_{\text{bub}} = \|\psi\|_e . \tag{3.20}$$

In what follows, we show how the lower bound estimate η^u_{bub} can be improved, by analyzing the difference $(\tilde{\varphi} - \psi) \in \tilde{V}^{h,p}$, which satisfies

$$B(\tilde{\varphi} - \psi, v) = \mathcal{R}^u_{h,p}(v) - B(\psi, v) , \quad \forall\, v \in \tilde{V}^{h,p} . \tag{3.21}$$

Then, using Eqs. (3.11) and (3.5), we have $B(\psi, \psi) = \mathcal{R}^u_{h,p}(\psi) = B(\tilde{\varphi}, \psi)$, so that

$$\|\tilde{\varphi}\|_e^2 = \|\psi\|_e^2 + \|\tilde{\varphi} - \psi\|_e^2 . \tag{3.22}$$

It immediately follows from Eq. (3.11) that $\mathcal{R}^u_{h,p}(v) - B(\psi, v) = 0$ for all $v \in W$; this suggests that one can find an approximation $\phi \in V^{h,p}$ of $(\tilde{\varphi} - \psi)$ satisfying

$$B(\phi, v) = \mathcal{R}^u_{h,p}(v) - B(\psi, v) , \quad \forall\, v \in V^{h,p} , \tag{3.23}$$

which simplifies to

$$B(\phi, v) = -B(\psi, v), \quad \forall v \in V^{h,p}, \tag{3.24}$$

since $\mathscr{R}^u_{h,p}(v) = 0$, for all $v \in V^{h,p}$. As before, we can relate the approximation ϕ to the function $\tilde{\varphi} - \psi$:

THEOREM 3.2. Let $\tilde{\varphi}$, ψ and ϕ be the solutions of (3.5), (3.11) and (3.24). Then, there exists a constant γ, $0 \leq \gamma \leq 1$ such that

$$\sqrt{(1-\gamma^2)}\|\tilde{\varphi} - \psi\|_e \leq \|\phi\|_e \leq \|\tilde{\varphi} - \psi\|_e . \tag{3.25}$$

PROOF. The proof is similar to the proof of Theorem 3.1. (We remark that the constant γ is not necessarily the same as in Theorem 3.1). □

From this theorem, it follows that

$$\|\psi\|_e^2 + (1-\gamma^2)\|\tilde{\varphi} - \psi\|_e^2 \leq \|\psi\|_e^2 + \|\phi\|_e^2 \leq \|\psi\|_e^2 + \|\tilde{\varphi} - \psi\|_e^2 , \tag{3.26}$$

which implies, using (3.22) and (3.9), that:

$$\sqrt{(1-\sigma^2)(1-\gamma^2)}\|\varphi\|_e \leq \sqrt{\|\psi\|_e^2 + \|\phi\|_e^2} \leq \|\varphi\|_e . \tag{3.27}$$

Again, this new global error estimator

$$\eta^u_{\text{low}} = \sqrt{\|\psi\|_e^2 + \|\phi\|_e^2} \tag{3.28}$$

provides a lower bound on $\|\varphi\|_e$. The cost of obtaining ϕ is limited to one forward and one backward substitution when problem (2.2) is solved using a direct method. Moreover, observing that there exists γ_{pol}, $0 \leq \gamma_{\text{pol}} < 1$, such that

$$B(\phi, \psi) = -\gamma_{\text{pol}}\|\phi\|_e\|\psi\|_e \tag{3.29}$$

we have, replacing v by ϕ in (3.24),

$$\|\phi\|_e^2 = B(\phi, \phi) = -B(\phi, \psi) = \gamma_{\text{pol}}\|\phi\|_e\|\psi\|_e \tag{3.30}$$

so that

$$\gamma_{\text{pol}} = \frac{\|\phi\|_e}{\|\psi\|_e} . \tag{3.31}$$

The ratio γ_{pol} provides us with valuable information regarding the quality of the error estimators η^u_{bub} and η^u_{low}. Indeed, it can be interpreted as an indicator of how much 'energy' is transmitted from the bubble functions in W (small scales) to the basis functions in $V^{h,p}$ (large scales). Since the propagation of information is enhanced among the large scales, the quantity γ_{pol} measures how the error is 'polluted' away from the sources of error. It is therefore called *pollution factor*. We have observed in numerical experiments that the smaller γ_{pol} is, the better the quality of the error estimators.

3.3. Upper bounds

We have seen earlier that to construct an upper bound of $\|\varphi\|_e$ (resp. $\|\tilde{\varphi}\|_e$), it is necessary to define a space larger than V (resp. $\tilde{V}^{h,p}$). We provide here a brief summary of the methodology proposed by Ainsworth and Oden [2].

First, for each element of the mesh Ω_K, one defines the local space $V(\Omega_K)$ (in the case $V = H^1_0(\Omega)$)

$$V(\Omega_K) = \{v \in H^1(\Omega_K);\ v = 0 \text{ on } \partial\Omega \cap \partial\Omega_K\} . \tag{3.32}$$

Then, we assemble the *broken space* $V(\mathscr{P}^h)$, $V \subset V(\mathscr{P}^h)$, associated with the mesh (or partition) $\mathscr{P}^h$, as:

$$V(\mathcal{P}^h) = \prod_K V(\Omega_K),$$

where Π_K denotes the product over all the elements of the mesh. Meanwhile, the residual $\mathcal{R}^u_{h,p}$ is extended to the linear functional $\hat{\mathcal{R}}^u_{h,p} : V(\mathcal{P}^h) \to \mathbb{R}$:

$$\hat{\mathcal{R}}^u_{h,p}(v) = \sum_K \mathcal{R}^u_{h,p,K}(v|_K) + \Gamma(v), \quad \forall\, v \in V(\mathcal{P}^h), \tag{3.33}$$

where

$$\mathcal{R}^u_{h,p,K}(v|_K) = F_K(v|_K) - B_K(u_{h,p}|_K, v|_K). \tag{3.34}$$

Here, $F_K(v|_K)$ and $B_K(v|_K, v|_K)$ represent the restrictions of $F(v)$ and $B(v, v)$ to element Ω_K of the mesh. Moreover, in (3.33), Γ denotes a linear functional defined on $V(\mathcal{P}^h)$ which vanishes on V so that

$$\hat{\mathcal{R}}^u_{h,p}(v) = \mathcal{R}^u_{h,p}(v), \quad \forall\, v \in V.$$

The functional Γ contains information about interelement boundaries. It is defined such that the global problem (3.3) is decoupled into a series of elementwise subproblems, while retaining the upper bound on $\|\varphi\|_e$. Moreover, it is chosen so that the local subproblems are all solvable, in the sense that the interelement fluxes are in *equilibrium* with respect to the data of each local residual problem. Then for each element $\Omega_K \in \mathcal{P}^h$, we solve for the function $\varphi_K \in V(\Omega_K)$ which satisfies the local problem:

$$B_K(\varphi_K, v) = \mathcal{R}^u_{h,p,K}(v) + \oint_{\partial\Omega_K} g_K v \, ds, \quad \forall\, v \in V(\Omega_K), \tag{3.35}$$

where g_K denotes the equilibrated flux for each element. At this point, one emphasizes that neither the definition of Γ nor the construction of the interelement fluxes is unique. Some equilibration methods have been proposed by Ladevèze and Leguillon [12] and Ainsworth and Oden [1,2]. Then Ainsworth and Oden have shown that:

$$\|\varphi\|_e^2 \leq \sum_K \|\varphi_K\|_{e,K}^2. \tag{3.36}$$

However, because the spaces $V(\Omega_K)$ have infinite dimension, the local problems (3.35) can only be, at best, approximated. Starting from the space $V^{h,p}$ it is straightforward to construct the corresponding local finite element spaces $\tilde{V}^{h,p}(\Omega_K)$ for each element of the mesh. Then, in the same manner as before, we compute the functions $\tilde{\varphi}_K \in \tilde{V}^{h,p}(\Omega_K)$ as finite element approximations of (3.35). It follows as well that

$$\|\tilde{\varphi}\|_e^2 \leq \sum_K \|\tilde{\varphi}_K\|_{e,K}^2. \tag{3.37}$$

Finally, the new error estimator η^u_{upp}:

$$\eta^u_{\text{upp}} = \sqrt{\sum_K \|\tilde{\varphi}_K\|_{e,K}^2} \tag{3.38}$$

provides an upper bound to the quantity $\|\tilde{\varphi}\|_e$ (but not necessarily to $\|\varphi\|_e$).

4. Goal-oriented error estimation

The object of goal-oriented error estimation is to provide engineers with a tool that can assess the accuracy of finite element solutions in specific measures other than the classical energy norm. We present here the general theory when the measure is given by a linear function of the solution, and apply it to the particular case of *pointwise error estimation.*

4.1. General theory

Let us suppose that we are interested in estimating the error with respect to the measure L, where L denotes a linear functional defined on the space V. Then, the error E in the quantity $L(u_{h,p})$ reads, due to the linearity of L:

$$E = L(u) - L(u_{h,p}) = L(u - u_{h,p}) = L(e)\,. \tag{4.1}$$

In consequence, the objective is to relate the quantity $L(e)$ to the source of error $\mathscr{R}^{u}_{h,p}$; in other words, we aim at finding a continuous linear function ω, if it exists, such that

$$L(e) = \omega(\mathscr{R}^{u}_{h,p})\,. \tag{4.2}$$

The function ω is called the *influence function* (analogous to Green's functions) with respect to the linear functional L as it indicates the influence of the residual on $L(e)$. It naturally belongs to the bidual of V. Since V is a Hilbert space, it is also a reflexive space, so that (4.2) becomes

$$L(e) = \mathscr{R}^{u}_{h,p}(\omega)\,, \tag{4.3}$$

where ω is identified with an element of V. Using relation (2.3), one gets

$$L(e) = B(e, \omega)\,. \tag{4.4}$$

Therefore, the equality above is necessarily satisfied whenever $\omega \in V$ is the solution of

$$B(v, \omega) = L(v)\,, \quad \forall\, v \in V\,. \tag{4.5}$$

This auxiliary problem is often referred to as the *dual problem*. From the *Lax–Milgram theorem*, the influence function ω exists and is unique in V. This problem is infinite dimensional in V, so one can at best find an approximation $\omega_{h,p}$, for instance, in the finite element space $V^{h,p}$, such that

$$B(v, \omega_{h,p}) = L(v)\,, \quad \forall\, v \in V^{h,p}\,. \tag{4.6}$$

First, we observe that the cost to solve for $\omega_{h,p}$ is almost negligible, as the finite system of equations, thanks to the symmetry of $B(\cdot,\cdot)$, has already been factorized once to calculate $u_{h,p}$. Thus, the cost reduces to one backward and one forward substitution. Unfortunately, $\omega_{h,p} \in V^{h,p}$ does not provide any valuable information on $L(e)$, since from (2.5),

$$B(e, \omega_{h,p}) = \mathscr{R}^{u}_{h,p}(\omega_{h,p}) = 0\,. \tag{4.7}$$

Nevertheless, using both (4.7) and (4.3), one gets

$$L(e) = \mathscr{R}^{u}_{h,p}(\omega) - \mathscr{R}^{u}_{h,p}(\omega_{h,p}) = \mathscr{R}^{u}_{h,p}(\omega - \omega_{h,p}) = \mathscr{R}^{u}_{h,p}(\varepsilon) = B(e, \varepsilon) \tag{4.9}$$

where $\varepsilon \in V$, $\varepsilon = \omega - \omega_{h,p}$, denotes the error in the influence function and is the solution of

$$B(v, \varepsilon) = \mathscr{R}^{\omega}_{h,p}(v)\,, \quad \forall\, v \in V\,. \tag{4.9}$$

Here, the linear functional $\mathscr{R}^{\omega}_{h,p}$ is the residual with respect to the error ε.

So far, we have been able to show the following relationships for $L(e)$, derived from (4.8) and (4.9),

$$L(e) = \mathscr{R}^{u}_{h,p}(\varepsilon) = B(e, \varepsilon) = \mathscr{R}^{\omega}_{h,p}(e)\,. \tag{4.10}$$

A new relation, inferred from a property of the inner product $B(\cdot,\cdot)$ [4], is given by

$$L(e) = B(e, \varepsilon) = B\left(se, \frac{\varepsilon}{s}\right) = \frac{1}{4}\left\| se + \frac{\varepsilon}{s}\right\|^2_e - \frac{1}{4}\left\| se - \frac{\varepsilon}{s}\right\|^2_e \tag{4.11}$$

where s defines an arbitrary scaling factor. The value of s is selected so that the quantities $\|se\|_e$ and $\|\varepsilon/s\|_e$ have the same amplitudes, i.e. $\|se\|_e = \|\varepsilon/s\|_e$, which implies that

$$s = \sqrt{\frac{\|\varepsilon\|_e}{\|e\|_e}}\,. \tag{4.12}$$

This particular choice of s represents a minimizer for the quantities $\|se + \varepsilon/s\|^2_e$ and $\|se - \varepsilon/s\|^2_e$.

The relationship (4.11) tells us that the error quantity $L(e)$ is expressed as the difference of the energy norms of two linear combinations of e and ε. We have described, in the last section, reliable techniques to obtain lower

and upper bounds of the errors in the energy norm. Let η^+_{low}, η^+_{upp}, η^-_{low} and η^-_{upp} be global error estimates such that:

$$\eta^+_{\text{low}} \leq \left\| se + \frac{\varepsilon}{s} \right\|_e \leq \eta^+_{\text{upp}} \tag{4.13}$$

$$\eta^-_{\text{low}} \leq \left\| se - \frac{\varepsilon}{s} \right\|_e \leq \eta^-_{\text{upp}} \tag{4.14}$$

It immediately follows, using (4.11), that

$$\frac{1}{4}(\eta^+_{\text{low}})^2 - \frac{1}{4}(\eta^-_{\text{upp}})^2 \leq L(e) \leq \frac{1}{4}(\eta^+_{\text{upp}})^2 - \frac{1}{4}(\eta^-_{\text{low}})^2 \tag{4.15}$$

which provides a *lower bound* and an *upper bound* for the error quantity $L(e)$.

In addition to the lower and upper bounds above, we also compute estimates η_L of the quantity $L(e)$ either by using the upper bounds η^-_{upp} and η^+_{upp}:

$$\eta_L = \frac{1}{4}(\eta^+_{\text{upp}})^2 - \frac{1}{4}(\eta^-_{\text{upp}})^2, \tag{4.16}$$

or by using the lower bounds η^-_{low} and η^+_{low}:

$$\eta_L = \frac{1}{4}(\eta^+_{\text{low}})^2 - \frac{1}{4}(\eta^-_{\text{low}})^2. \tag{4.17}$$

or by using the averages:

$$\eta_L = \frac{1}{8}\{(\eta^+_{\text{low}})^2 + (\eta^+_{\text{upp}})^2\} - \frac{1}{8}\{(\eta^-_{\text{low}})^2 + (\eta^-_{\text{upp}})^2\}, \tag{4.18}$$

In all cases, we observe that

$$\frac{1}{4}(\eta^+_{\text{low}})^2 - \frac{1}{4}(\eta^-_{\text{upp}})^2 \leq \eta_L \leq \frac{1}{4}(\eta^+_{\text{upp}})^2 - \frac{1}{4}(\eta^-_{\text{low}})^2. \tag{4.19}$$

REMARK 1. In order to calculate the bounds η^+_{low}, η^+_{upp}, η^-_{low} and η^-_{upp}, we actually compute the approximations ψ^e, ϕ^e and $\tilde{\varphi}^e_K$ with respect to the error e, solving (3.11), (3.24) and (3.35), respectively, and the approximations ψ^ε, ϕ^ε and $\tilde{\varphi}^\varepsilon_K$ with respect to ε, solving the same problems as before using the residual $\mathscr{R}^\omega_{h,p}$ instead of $\mathscr{R}^u_{h,p}$. We then calculate the upper estimates η^u_{upp} and η^ω_{upp}

$$\eta^u_{\text{upp}} = \sqrt{\sum_K \|\tilde{\varphi}^e_K\|^2_{e,K}} \tag{4.20}$$

$$\eta^\omega_{\text{upp}} = \sqrt{\sum_K \|\tilde{\varphi}^\varepsilon_K\|^2_{e,K}} \tag{4.21}$$

in order to obtain an approximation $\bar{s}$ of the scaling factor s:

$$\bar{s} = \sqrt{\frac{\eta^\omega_{\text{upp}}}{\eta^u_{\text{upp}}}}. \tag{4.22}$$

Moreover, since all the problems involved in computing ψ^e, ϕ^e, $\tilde{\varphi}^e_K$ and ψ^ε, ϕ^ε, $\tilde{\varphi}^\varepsilon_K$ are linear, it suffices to compute the linear combinations of these functions to obtain the global quantities:

$$\eta^-_{\text{low}} = \sqrt{\|\bar{s}\psi^e - \bar{s}^{-1}\psi^\varepsilon\|^2_e + \|\bar{s}\phi^e - \bar{s}^{-1}\phi^\varepsilon\|^2_e} \tag{4.23}$$

$$\eta^+_{\text{low}} = \sqrt{\|\bar{s}\psi^e + \bar{s}^{-1}\psi^\varepsilon\|^2_e + \|\bar{s}\phi^e + \bar{s}^{-1}\phi^\varepsilon\|^2_e} \tag{4.24}$$

$$\eta^-_{\text{upp}} = \sqrt{\sum_K \|\bar{s}\tilde{\varphi}^e_K - \bar{s}^{-1}\tilde{\varphi}^\varepsilon_K\|^2_{e,K}} \tag{4.25}$$

$$\eta^{+}_{\text{upp}} = \sqrt{\sum_K \|\bar{s}\tilde{\varphi}^e_K + \bar{s}^{-1}\tilde{\varphi}^e_K\|^2_{e,K}} \tag{4.26}$$

REMARK 2. We note that the approach of Paraschivoiu and Patera [16], applied to symmetric positive-definite problems, would amount to considering bounds of the form:

$$-\frac{1}{4}(\eta^{-}_{\text{upp}})^2 \leq L(e) \leq \frac{1}{4}(\eta^{+}_{\text{upp}})^2 . \tag{4.27}$$

These bounds are less expensive to obtain, since only the estimates η^{-}_{upp} and η^{+}_{upp} are needed. On the other hand, they are obviously less sharp than those in (4.15). However, the effectivity indices they present in numerical experiments are very close to one, since these are determined with respect to the quantity of interest $L(u)$ (and not $L(e)$), for which they compute the bounds:

$$L(u_{h,p}) - \frac{1}{4}(\eta^{-}_{\text{upp}})^2 \leq L(u) \leq L(u_{h,p}) + \frac{1}{4}(\eta^{+}_{\text{upp}})^2, \tag{4.28}$$

where u refers to the finite element solution on a very fine mesh.

4.2. Pointwise error estimation

In this section, we consider the particular case of pointwise error estimation. We suppose that the main goal of our numerical simulations is to obtain an 'accurate' value of the solution u at a given point $\boldsymbol{x}_0 \in \bar{\Omega}$. From a mathematical point of view, it is known, in the case where $u \in V = H^1(\Omega)$, that the solution may not be continuous when the geometrical dimension d is equal to or higher than two, which implies that $u(\boldsymbol{x}_0)$ may not be defined. We appeal here to the use of *mollification* (see [14, Chap. 2]) in order to circumvent this issue, which allows us to introduce the following quantity of interest

$$L_\epsilon(u;\boldsymbol{x}_0) = \int_\Omega u(\boldsymbol{x}) k_\epsilon(\boldsymbol{x}-\boldsymbol{x}_0)\,\mathrm{d}x \tag{4.29}$$

where the mollifiers k_ϵ form a family of infinitely smooth functions in $(-\infty,\infty)^d$ characterized by the parameter ϵ.

This approach is also well suited to estimate the pointwise error in the first derivatives of the solution, since pointwise derivatives are generally not defined at the element interfaces for the finite element solution $u_{h,p} \in V^{h,p}$. Supposing we are interested in the partial derivative of u with respect to the variable x, we may consider the following quantity of interest:

$$L_\epsilon(u;\boldsymbol{x}_0) = \int_\Omega \frac{\partial u}{\partial x}(\boldsymbol{x}) k_\epsilon(\boldsymbol{x}-\boldsymbol{x}_0)\,\mathrm{d}x . \tag{4.30}$$

The mollifying process can be viewed as an averaging of the quantity u or $\partial u/\partial x$ over a small neighborhood of the point $\boldsymbol{x}_0$.

It is customary (see [14, Chap. 2]) to choose the mollifiers k_ϵ of the form:

$$k_\epsilon(\boldsymbol{x}) = \begin{cases} C \exp -\dfrac{\epsilon^2}{\epsilon^2 - |\boldsymbol{x}|^2} & \text{if } |\boldsymbol{x}| < \epsilon \\ 0 & \text{if } |\boldsymbol{x}| \geq \epsilon \end{cases} \tag{4.31}$$

where the constant C, which depends on d, ϵ and $\boldsymbol{x}_0$, is selected to satisfy

$$\int_\Omega k_\epsilon(\boldsymbol{x}-\boldsymbol{x}_0)\,\mathrm{d}x = 1 . \tag{4.32}$$

Examples of mollifying functions k_ϵ are shown in Fig. 1 for various values of ϵ with $d = 1$.

In the following discussion, the quantity of interest $L_\epsilon(\cdot;\boldsymbol{x}_0)$ is taken to be the linear functional defined in (4.29). From the property (4.32) of mollifiers, we distinguish between the following two cases, depending on the location of $\boldsymbol{x}_0$ inside $\bar{\Omega}$:

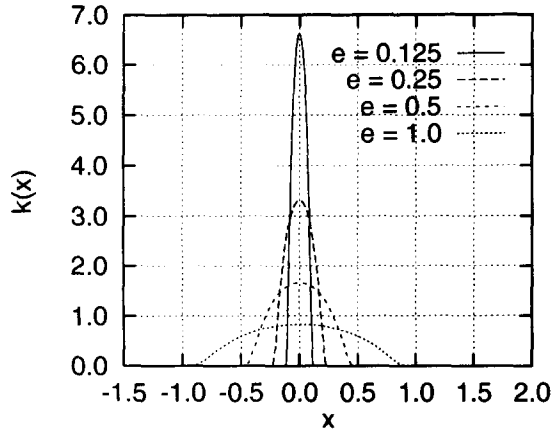

Fig. 1. Mollifiers $k_\epsilon(x)$ for $\epsilon = 1.0, 0.5, 0.25, 0.125$ in dimension $d = 1$.

(1) The point $\boldsymbol{x}_0$ is an 'interior' point, in the sense that the support of the mollifier, $\operatorname{supp} k_\epsilon(\boldsymbol{x} - \boldsymbol{x}_0)$, lies inside Ω. In this case, property (4.32) implies that the quantity $L_\epsilon(u; \boldsymbol{x}_0)$ is equal to $u(\boldsymbol{x}_0)$ for every value of ϵ whenever the function is constant or linear on Ω. Moreover, provided that $\boldsymbol{u}$ is continuous in the neighborhood of $\boldsymbol{x}_0$, $L_\epsilon(u; \boldsymbol{x}_0)$ converges to $u(\boldsymbol{x}_0)$ as ϵ tends to zero. Also, the value of the constant C is the same for all interior points of Ω and thus needs to be evaluated only once. Indeed, when $d = 1$, we have

$$\int_\Omega k_\epsilon(x - x_0)\,\mathrm{d}x = \int_{x_0+\epsilon}^{x_0+\epsilon} k_\epsilon(x - x_0)\,\mathrm{d}x = \epsilon C \int_{-1}^{+1} \exp\left(-\frac{1}{1-x^2}\right)\mathrm{d}x = 1$$

A numerical integration of the last integral provides the value 0.4440 so that $C \approx 2.2523\epsilon^{-1}$. If $d = 2$, we obtain $C \approx 2.1436\epsilon^{-2}$.

(2) The point $\boldsymbol{x}_0$ is a point close to the boundary in the sense that $(\operatorname{supp} k_\epsilon(\boldsymbol{x} - \boldsymbol{x}_0))\backslash(\operatorname{supp} k_\epsilon(\boldsymbol{x} - \boldsymbol{x}_0) \cap \Omega) \neq \emptyset$. This time, the quantity $L_\epsilon(u; \boldsymbol{x}_0)$ is equal to $u(\boldsymbol{x}_0)$ when u is constant, but not necessarily equal when it is a linear function. Nevertheless, $L_\epsilon(u; \boldsymbol{x}_0)$ still converges to $u(\boldsymbol{x}_0)$ as ϵ tends to zero whenever u is continuous in a neighborhood of $\boldsymbol{x}_0$. On the other hand, the value of the constant C varies with the distance of $\boldsymbol{x}_0$ from the boundary $\partial\Omega$.

REMARK 3. Because of the second case above, we decide to approximate the constant C by integrating (4.32) numerically using the finite element method.

REMARK 4. From a numerical point of view, it is convenient to define quantity of interest L in the form of an integral, since integration is at the heart of all finite element codes. However, integration is generally carried out using classical Gauss quadrature rules, and accuracy is directly correlated to the number of Gaussian points used in each element. Therefore, it appears necessary to limit the size of the support of $k_\epsilon(\boldsymbol{x} - \boldsymbol{x}_0)$, equal to 2ϵ, with respect to the mesh size h of the element containing the point $\boldsymbol{x}_0$. Therefore, one requires that

$$\kappa \leqslant \frac{2\epsilon}{h} \tag{4.33}$$

or $\epsilon \geqslant h\kappa/2$, where κ is a given fractional number. In order to attain an acceptable accuracy for L while avoiding too many Gaussian points, we suggest the value $\kappa = 1/4$.

Finally, we introduce the effectivity index λ_e in order to evaluate the accuracy of $L_\epsilon(e; \boldsymbol{x}_0)$ with respect to $e(\boldsymbol{x}_0)$ (whenever $e(\boldsymbol{x}_0)$ is defined and not equal to 0):

$$\lambda_e = \frac{L_\epsilon(e; \boldsymbol{x}_0)}{e(\boldsymbol{x}_0)}, \tag{4.34}$$

where the subscript in λ_ε is used to emphasize that the effectivity index is dependent on the value of ϵ. A similar analysis holds for the estimation of error in the first derivative of the solution.

5. Strategy towards pointwise error control

The strategy employed to control the pointwise error $L_\epsilon(e;x_0)$ at a point x_0, with L_ϵ given in (4.29) or in (4.30), consists of two steps:

(1) Compute the finite element solution $u_{h,p}$, and the error estimate η_L of (4.16) for $L_\epsilon(e;x_0)$. Check whether the relative error is smaller than a preset tolerance C^{tol}.

(2) If the tolerance is not achieved, adapt the finite element mesh in order to reduce the effects of the sources of errors.

The relative error is commonly defined as $e_{\text{rel}} = |L_\epsilon(e;x_0)|/|L_\epsilon(u;x_0)|$. Since both the exact solution and error are unknown, we use the available approximations instead. Then, the mesh needs to be adapted whenever

$$\frac{|\eta_L|}{|L_\epsilon(u_{h,p};x_0)|} \geq C^{\text{tol}}. \tag{5.1}$$

Adaptation of the mesh is accomplished by refining the elements which contribute to $L_\epsilon(e;x_0)$ the most. Using relation (4.10), one immediately observes that

$$|L_\epsilon(e;x_0)| = |B(e,\varepsilon)| \leq \sum_K |B_K(e,\varepsilon)| \leq \sum_K \|e\|_{e,K}\|\varepsilon\|_{e,K}. \tag{5.2}$$

Let $\eta^u \approx \|e\|_e$ and $\eta^\omega \approx \|\varepsilon\|_e$ be any of the global estimators presented in Section 3. We decompose these into elementwise quantities

$$(\eta^u)^2 = \sum_K (\eta_K^u)^2, \quad (\eta^\omega)^2 = \sum_K (\eta_K^\omega)^2, \tag{5.3}$$

Then, an element Ω_K of the mesh is refined if

$$\frac{\eta_K^u \cdot \eta_K^\omega}{\max_J(\eta_J^u \cdot \eta_J^\omega)} \geq C^{\text{adp}}. \tag{5.4}$$

Here, C^{adp} is a user-defined parameter ranging between 0 and 1.

6. Numerical example

Here, we apply the theoretical results presented in the previous sections to a one-dimensional problem. The problem consists of solving for the smooth solution u, defined on the unit interval $\Omega = (0,1)$, which satisfies the ordinary differential equation:

$$-\frac{\mathrm{d}}{\mathrm{d}x}\left(a(x)\frac{\mathrm{d}u}{\mathrm{d}x}\right) + b(x)u = f(x), \quad \forall x \in (0,1), \tag{6.1}$$

subject to the boundary conditions:

$$u(0) = 0, \qquad a(1)\frac{\mathrm{d}u}{\mathrm{d}x}(1) = 0. \tag{6.2}$$

The coefficients a and b are given by

$$a(x) = 1 + 9\exp - \frac{(x-0.5)^2}{0.025^2}$$

$$b(x) = 1$$

and f is such that the exact solution $u \in V = \{v \in H^1(0,1);\ v(0) = 0\}$ reads

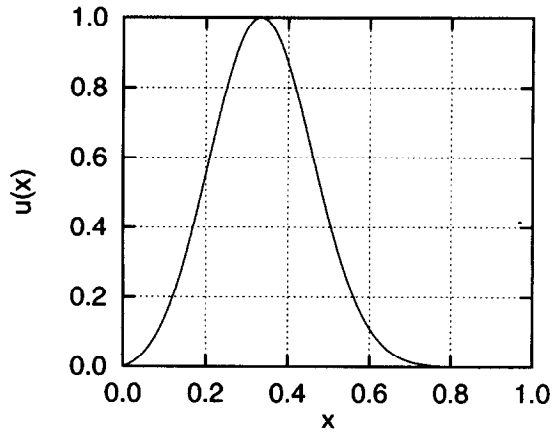

Fig. 2. Graph of exact solution $u(x)$ given in (6.3).

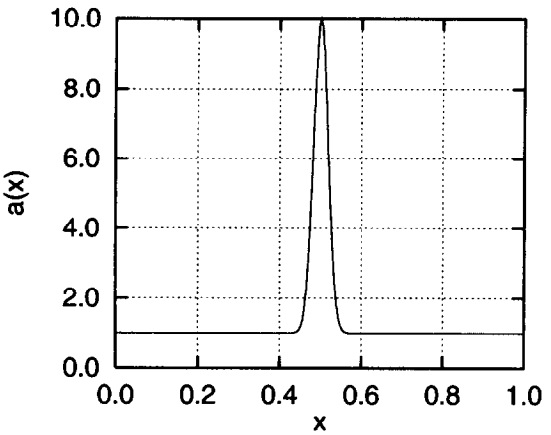

Fig. 3. Graph of coefficient $a(x)$.

$$u(x) = \frac{27}{4} x(1-x)^2 \exp - \frac{(x-1/3)^2}{0.04}. \tag{6.3}$$

The graphs of the solution $u(x)$ and of the data $a(x)$ are shown in Figs. 2 and 3.

In the first series of experiments, we briefly study the quality of the global error estimators η^u_{bub}, η^u_{low} and η^u_{upp}. The unit interval is discretized into a uniform mesh with mesh size $h = 1/N_e$, where N_e denotes the number of elements. The polynomial degree p for the approximations $u_{h,p}$ is also chosen uniform over the mesh. Moreover, we uniformly set $q = 2$ so that the bubble functions of W are the basis functions of degree $p+1$ and $p+2$. As usual, we measure the quality of the estimators by effectivity indices

$$\lambda = \frac{\eta^u}{\|e\|_e}, \tag{6.4}$$

where η^u denotes one of the estimators. The effectivity indices are shown in Fig. 4 in the case the solution $u_{h,p}$ is computed with $p = 1$ and in Fig. 6 with $p = 2$. We show the associated pollution factor γ_{pol} in Fig. 5 and Fig. 7, respectively.

In both cases, we observe that the upper bound estimate η^u_{upp} is more accurate than the lower bound estimate η^u_{low}, but the latter also becomes very accurate as the pollution factor γ_{pol} gets closer to zero. Not surprisingly, the value of γ_{pol} decreases as the number of degrees of freedom is increased and becomes very small in the asymptotic range. This can be attributed to the localization of the effects of the residual in the asymptotic range.

The second set of experiments is devoted to the study of pointwise error estimation. We therefore utilize the

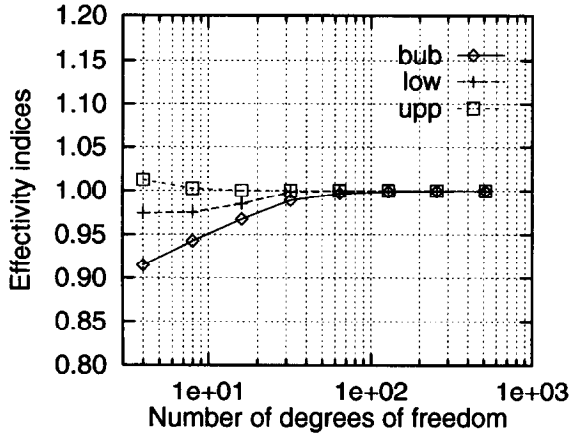

Fig. 4. Effectivity indices for the error estimates η^u_{bub} (1), η^u_{low} (2) and η^u_{upp} (3) in the case $p = 1$.

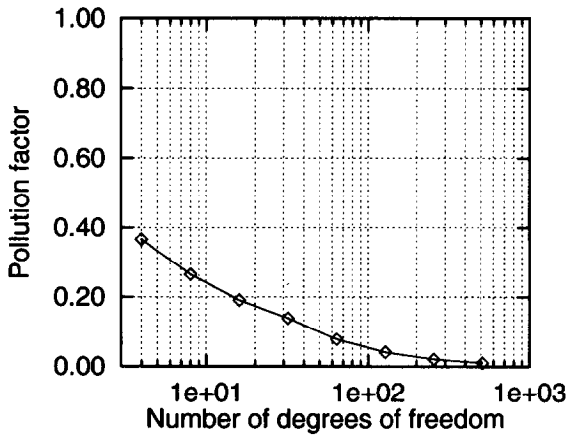

Fig. 5. Pollution factor γ_{pol} in the case $p = 1$.

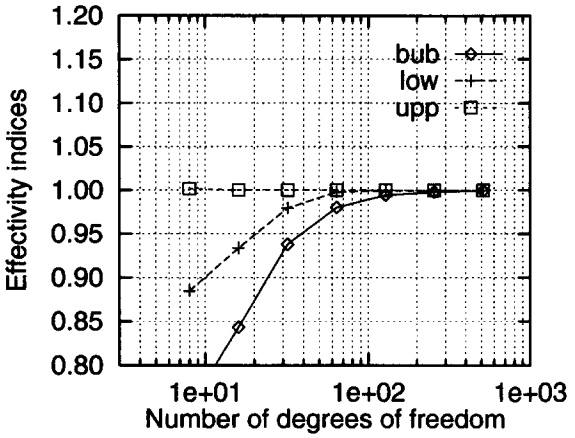

Fig. 6. Effectivity indices for the error estimates η^u_{bub} (1), η^u_{low} (2) and η^u_{upp} (3) in the case $p = 2$.

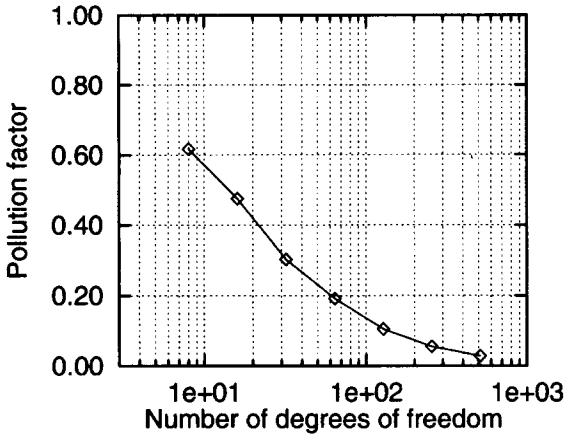

Fig. 7. Pollution factor γ_{pol} in the case $p = 2$.

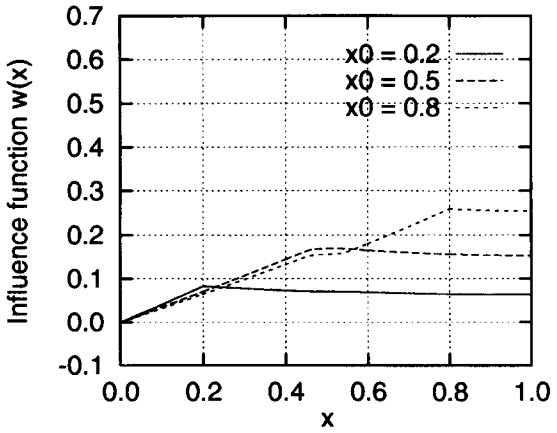

Fig. 8. Examples of influence functions with respect to the pointwise values at various locations x_0.

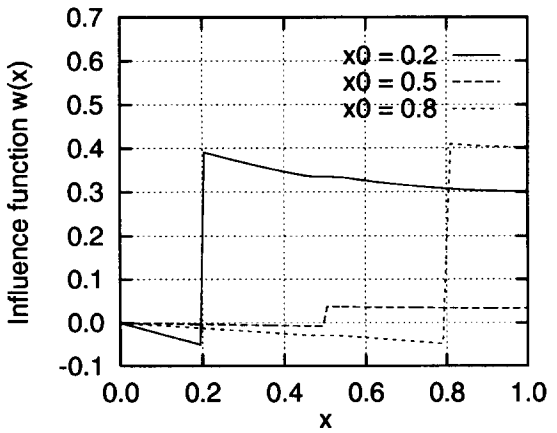

Fig. 9. Examples of influence functions with respect to the pointwise derivatives at various locations x_0.

linear functional $L_\epsilon(\cdot; x_0)$ defined in (4.29) for pointwise values of u at the point x_0 in [0, 1], and the functional $L_\epsilon(\cdot; x_0)$ defined in (4.30) for the pointwise derivatives at x_0. Beforehand, we plot in Figs. 8 and 9 examples of influence functions ω computed with respect to the pointwise values $u(x_0)$ and $\mathrm{d}u/\mathrm{d}x(x_0)$, respectively, at the locations $x_0 = 0.2$, 0.5 and 0.8.

We now explore the influence of the parameter ϵ with respect to the mesh size h on the effectivity index λ_e defined in (4.34). In order to do so, we construct uniform meshes of mesh size h for which we can compute the exact quantities $L_\epsilon(e; x_0)$ and $e(x_0)$. We then determine ϵ in such a way that the parameter κ

$$\kappa = \frac{2\epsilon}{h}$$

takes on the values 1, 1/2, 1/4 and 1/8. We remark here that the integration of $L_\epsilon(e; x_0)$ is performed using fifteen Gaussian points and that the solutions $u_{h,p}$ are piecewise linear, i.e. $p = 1$. The effectivity indices for $x_0 = 0.3333$ and $x_0 = 0.6$ are shown in Figs. 10 and 11, respectively. In the first case, we observe that the graph of the effectivity index converges to the line $\eta = 1$ for all meshes as κ takes on successive values of 1, 1/2 and 1/4. Then, when κ is equal to 1/8, the index deteriorates (the graph moves away from $\eta = 1$) because the number of integration points that fall inside the support of k_ϵ becomes too small. For the case $x_0 = 0.6$, we notice the same tendency. However, the effectivity index exhibits a sawtooth behavior as the mesh is refined. In the following experiments, we will use $\epsilon = h/8$, corresponding to $\kappa = 1/4$, where h is the size of the element containing x_0.

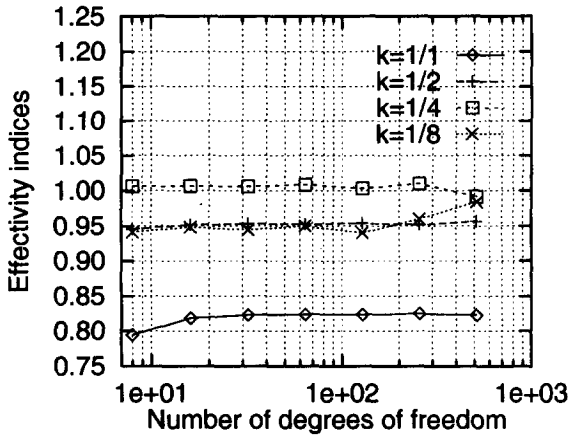

Fig. 10. Effectivity indices λ_ϵ obtained on uniform meshes using $\kappa = 1, 1/2, 1/4, 1/8$ for the quantity $u(0.3333)$.

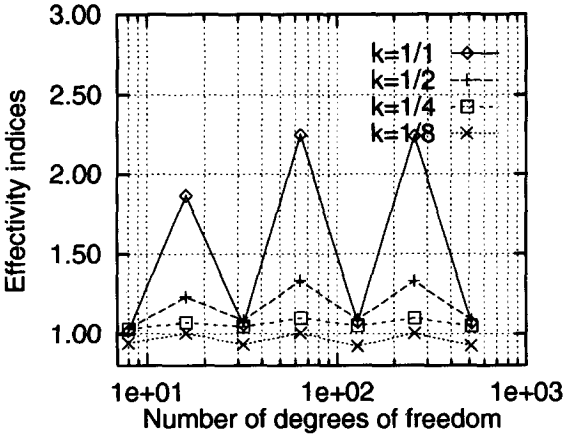

Fig. 11. Effectivity indices λ_ϵ obtained on uniform meshes using $\kappa = 1, 1/2, 1/4, 1/8$ for the quantity $u(0.6)$.

We now proceed by estimating the pointwise error in the solution $u_{h,p}$ at the points $x_0 = 0.3333$ and $x_0 = 0.8750$. We select the first point because it is in the neighborhood of the point where the solution u reaches its maximum on the interval (0, 1), and the second point because it lies in the region where the error is mainly composed of 'pollution' error due to the stiffness of the coefficient $a(x)$ at $x = 0.5$ and to the natural boundary condition at $x = 1$. The finite element solutions are computed with $p = 1$ and the errors estimated with $q = 2$. We then calculate effectivity indices for the lower and upper bounds (4.15) and for the estimate η_L (4.16) with respect to $L_\epsilon(e; x_0)$. These effectivity indices versus the number of degrees of freedom are shown for $x_0 = 0.3333$ in Figs. 12 and 13 in the cases of uniform and adaptive mesh refinement, respectively. We note that the adaptive meshes are constructed according to the strategy described in Section 5 using $C^{\text{adp}} = 0.2$. In both cases, the effectivity index for the estimate η_L remains close to one when the number of degrees of freedom becomes large enough. On the other hand, the effectivity indices for the bounds provide more accurate results in the case of uniform refinement. However, we observe in Fig. 14 that the relative error is smaller by several orders of magnitude for the adaptive refinement. This reveals that refinement needs to be essentially local to control the pointwise error at $x_0 = 0.3333$. Values of the effectivity index λ_ϵ are shown in Fig. 15.

We repeat the experiments for the case $x_0 = 0.8750$ and the same set of results are shown in Figs. 16–19. This time however, we observe that the relative error in the case of adaptive refinement is only smaller by one order of magnitude than that obtained by uniform refinement. This implies that more elements far from the point

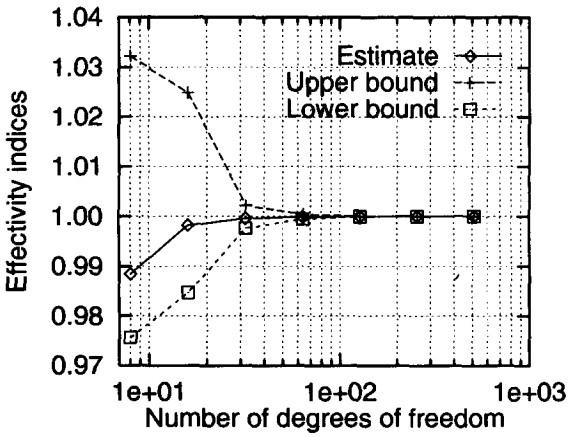

Fig. 12. Effectivity indices of the estimates and bounds for the quantity $u(0.3333)$ with uniform refinement.

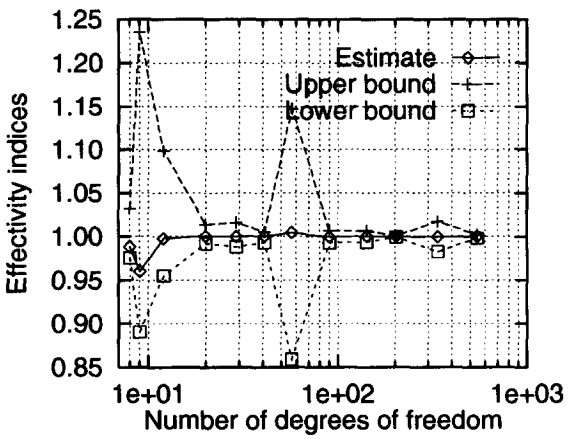

Fig. 13. Effectivity indices of the estimates and bounds for the quantity $u(0.3333)$ with adaptive refinement.

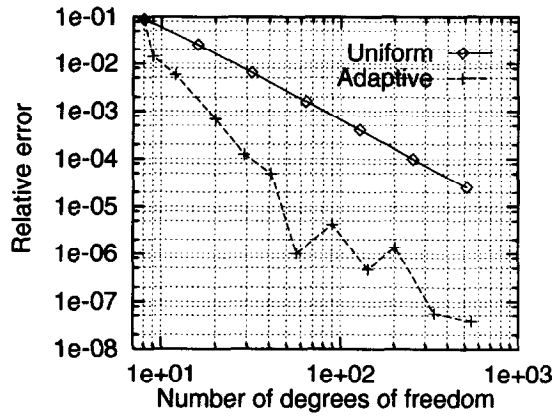

Fig. 14. Comparison of the evolution of the relative error using uniform and adaptive refinement for $u(0.3333)$.

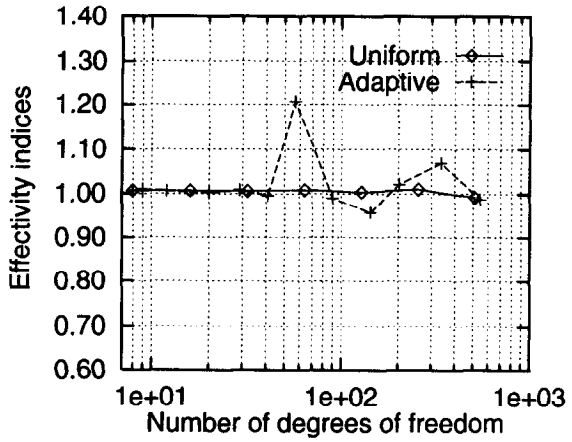

Fig. 15. Effectivity indices λ_e for the quantity $u(0.3333)$.

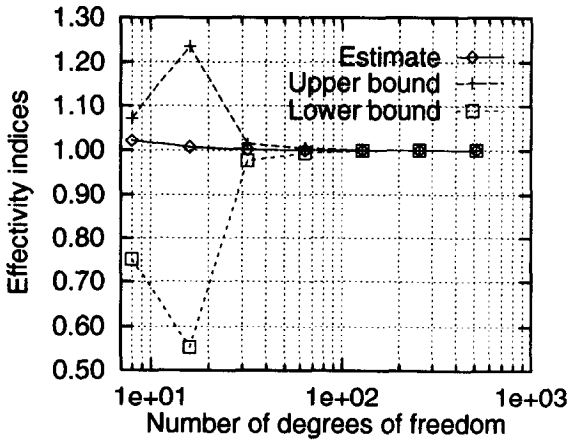

Fig. 16. Effectivity indices of the estimates and bounds for the quantity $u(0.8750)$ with uniform refinement.

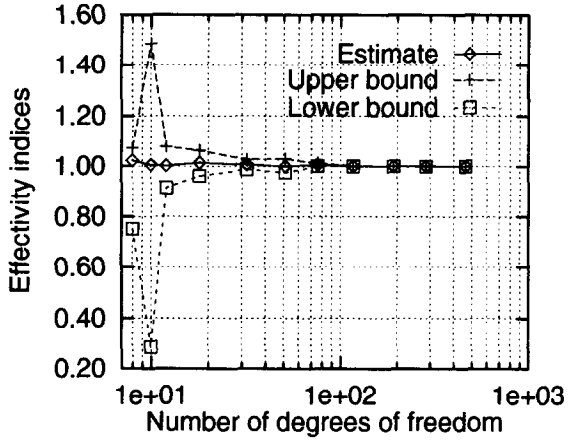

Fig. 17. Effectivity indices of the estimates and bounds for the quantity $u(0.8750)$ with adaptive refinement.

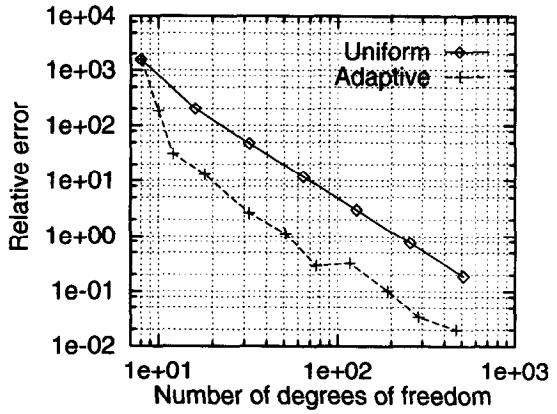

Fig. 18. Comparison of the evolution of the relative error using uniform and adaptive refinement for $u(0.8750)$.

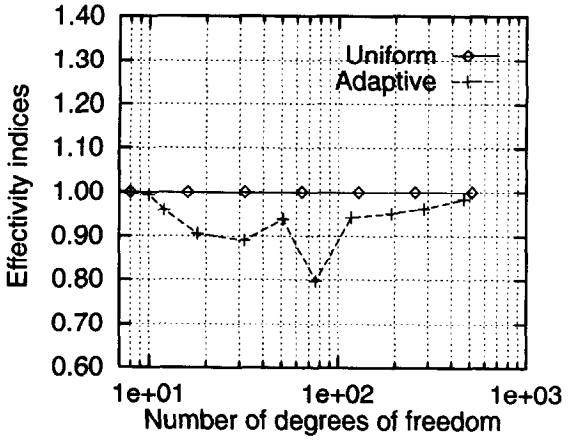

Fig. 19. Effectivity indices λ_e for the quantity $u(0.8750)$.

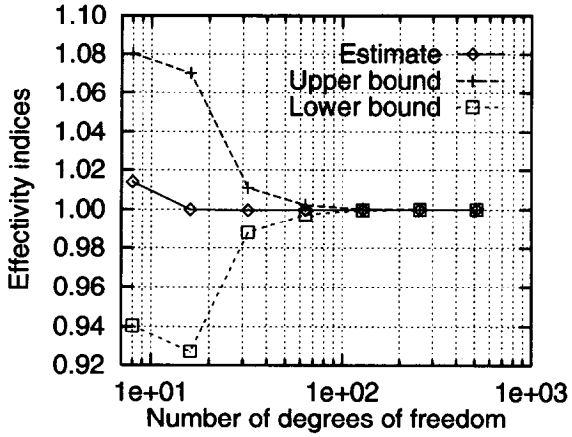

Fig. 20. Effectivity indices of the estimates and bounds for the quantity $du/dx(0)$ with uniform refinement.

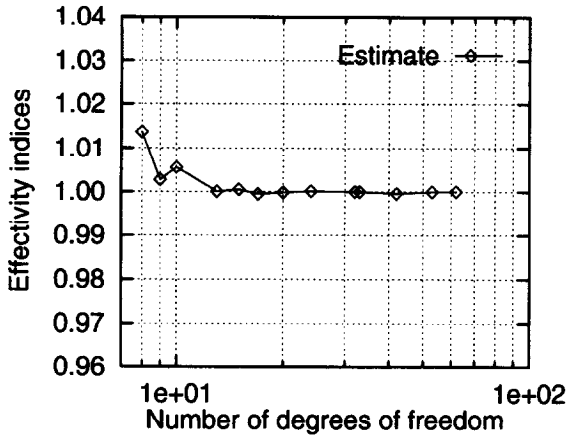

Fig. 21. Effectivity index of the estimate η_L for the quantity $du/dx(0)$ with adaptive refinement.

$x_0 = 0.8750$ need to be refined in order to control the pointwise error, which confirms that the pollution component of the error is predominant in $e(0.8750)$.

The goal of the next set of experiments is to evaluate the accuracy of the pointwise derivative du/dx at the boundary point $x_0 = 0$. We recall that the quantity of interest reads in this case:

$$L_\epsilon(u;0) = \int_\Omega \frac{du}{dx}(x) k_\epsilon(x)\, dx\,. \tag{6.5}$$

This time, the effectivity indices of the estimate η_L and of the lower and upper bounds, shown in Fig. 20 when the mesh is uniformly refined, are still very accurate. However, when the mesh is adaptively refined, the effectivity indices of the bounds, shown in Fig. 22, vary between -1 and $+3$, while the effectivity index for the estimate η_L remains very close to 1 as shown in Fig. 21. This is partially explained by the fact that the quantities η^-_{low}, η^+_{low}, η^-_{upp} and η^+_{upp}, in the case of adaptive refinement, become much larger than the quantity $L_\epsilon(e;)$ itself. Since the lower bounds η^-_{low}, η^+_{low} and upper bounds η^-_{upp}, η^+_{upp} are obtained by two different methods, the differences $(\eta^+_{\text{low}})^2 - (\eta^-_{\text{upp}})^2$ and $(\eta^+_{\text{upp}})^2 - (\eta^-_{\text{low}})^2$ may take on large values. On the other hand, the estimate $\eta_L = (\eta^+_{\text{upp}})^2/4 - (\eta^-_{\text{upp}})^2/4$ may benefit from the cancellation of similar defects in the estimates. Additional investigation is needed to understand this phenomenon. It is worth noting though the excellent performance of the adaptive strategy towards the control of the pointwise error $de/dx(0)$ in view of Fig. 23.

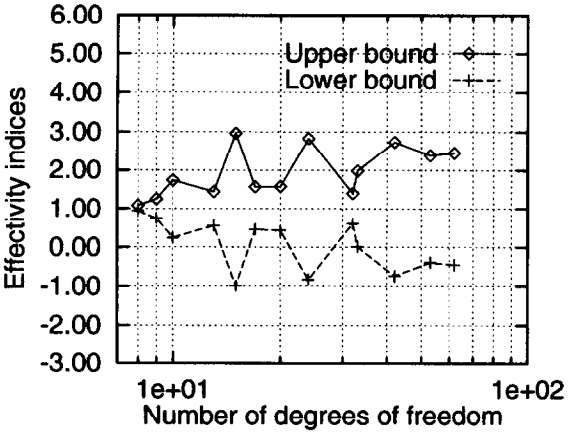

Fig. 22. Effectivity indices of the bounds for the quantity $du/dx(0)$ with adaptive refinement.

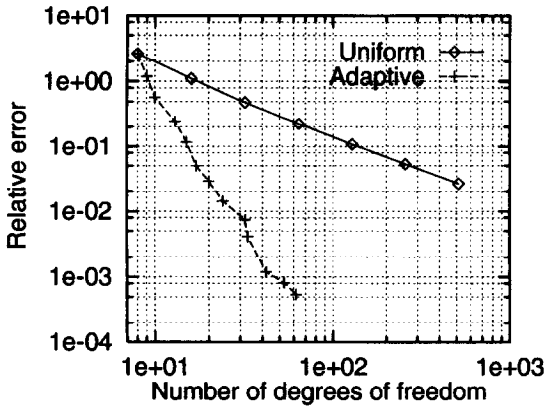

Fig. 23. Comparison of the evolution of the relative error using uniform and adaptive refinement for $du/dx(0)$.

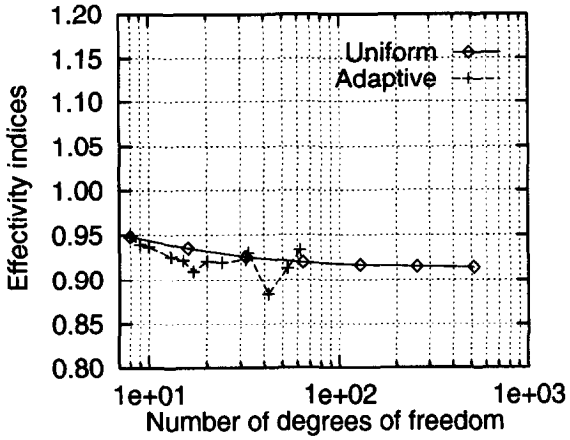

Fig. 24. Effectivity indices λ_ϵ for the quantity $du/dx(0)$.

Conclusions

We have presented a general theory for goal-oriented error estimation in the case of elliptic problems. We have shown that the method delivers not only an estimate of the error measured in terms of a specific quantity of interest but also lower and upper bounds which provide an interval of confidence for the estimate itself. The methodology has been successfully applied to estimate pointwise errors in the finite element solution of a one-dimensional elliptic problem. It also allows one to optimize the number of degrees of freedom employed with respect to specific goals, the goal here being the control of the error at a given point of the computational domain. In view of these promising results, the authors plan to investigate the performance of the method on two-dimensional problems, to analyze the behavior for various linear functionals of general interest, and to extend the methodology to other classes of problems.

Acknowledgment

The support of this work by the Office of Naval Research under contract N00014-95-1-0401 and by a grant from the Ford Motor Co. is gratefully acknowledged.

References

[1] M. Ainsworth and J.T. Oden, A unified approach to a posteriori error estimation using element residual methods, Numer. Math. 65 (1993) 23–50.

[2] M. Ainsworth and J.T. Oden, A posteriori error estimation in finite element analysis, Comput. Methods Appl. Mech. Engrg. 142 (1997) 1–88.

[3] I. Babuška and W. Rheinboldt, A posteriori error estimates for the finite element method, Int. J. Numer. Methods Engrg. 12 (1978) 1597–1615.

[4] I. Babuška, T. Strouboulis, K. Copps, S.K. Gangaraj and C.S. Upadhyay, A-posteriori error estimation for finite element and generalized finite element method, TICAM Report 98-01, The University of Texas at Austin, 1998.

[5] R.E. Bank, Hierarchical bases and the finite element method, Acta Numerica 5 (1996) 1–43.

[6] R.E. Bank and R.K. Smith, A posteriori error estimates based on hierarchical bases, SIAM J. Numer. Anal. 30 (1993) 921–935.

[7] R.E. Bank and A. Weiser, Some a posteriori error estimates for elliptic partial differential equations, Math. Comput. 44 (1985) 283–301.

[8] R. Becker and R. Rannacher, A feedback approach to error control in finite elements methods: Basic analysis and examples, preprint 96-52, Institut für Angewandte Mathematik, Universität Heidelberg, 1996, Comput Mech., to appear.

[9] R. Becker and R. Rannacher, Weighted a posteriori error control in FE method, in: ENUMATH-95, Paris, Sept. 1995.

[10] L. Demkowicz, J.T. Oden, W. Rachowicz and O. Hardy, Toward a universal *h-p* adaptive finite element strategy. Part 1. Constrained approximation and data structure, Comput. Methods Appl. Mech. Engrg. 77 (1989) 113–180.

[11] A. Huerta, P. Díez, A. Rodríguez-Ferran and G. Pijaudier-Cabot, Error estimation and adaptive finite element analysis of softening solids, in: P. Ladevèze and J.T. Oden, eds., Advances in Adaptive Computational Methods in Mechanics (Elsevier, Amsterdam, 1998) 333–347.

[12] P. Ladevèze and D. Leguillon, Error estimate procedure in the finite element method and applications, SIAM J. Numer. Anal. 20 (1983) 485–509.

[13] J.T. Oden and S. Prudhomme, A technique for a posteriori error estimation of *h-p* approximations of the Stokes equations, in: P. Ladevèze and J.T. Oden, eds., Advances in Adaptive Computational Methods in Mechanics (Elsevier, Amsterdam, 1998) 43–63.

[14] J.T. Oden and J.N. Reddy, An Introduction to the Mathematical Theory of Finite Elements (John Wiley & Sons, 1976).

[15] M. Paraschivoiu and A.T. Patera, A hierarchical duality approach to bounds for the outputs of partial differential equations, Comput. Methods Appl. Mech. Engrg. 158 (1998) 389–407.

[16] M. Paraschivoiu, J. Peraire and A.T. Patera, A posteriori finite element bounds for linear-functional outputs of elliptic partial differential equations, Comput. Methods Appl. Mech. Engrg. 150 (1997) 289–312.

[17] J. Peraire and A.T. Patera, Bounds for linear-functional outputs of coercive partial differential equations: local indicators and adaptive refinement, in: P. Ladevèze and J.T. Oden, eds., Advances in Adaptive Computational Methods in Mechanics (Elsevier, Amsterdam, 1998) 199–215.

[18] R. Rannacher and F.T. Stuttmeier, A posteriori error control in finite element methods via duality techniques: Application to perfect elasticity, Preprint 97-16, Institut für Angewandte Mathematik, Universität Heidelberg, 1997, Comput. Mech., to appear.

[19] R. Verfürth, A Review of A Posteriori Error Estimation and Adaptive Mesh-refinement Techniques (Wiley-Teubner, 1996).

[20] O.C. Zienkiewicz and J.Z. Zhu, The superconvergent patch recovery and a posteriori error estimates. Part 1: the recovery technique, Int. J. Numer. Methods Engrg. 33 (1992) 1331–1364.

[21] O.C. Zienkiewicz and J.Z. Zhu, The superconvergent patch recovery and a posteriori error estimates. Part 2: error estimates and adaptivity, Int. J. Numer. Methods Engrg. 33 (1992) 1365–1382.